https://doi.org/10.5194/egusphere-2024-2214
Preprint. Discussion started: 4 September 2024

Evaluating Arctic Sea-Ice and Snow Thickness: A Proxy-Based Comparison of MOSAiC Data with CMIP6 Simulations

Shreya Trivedi[1], Imke Sievers[2], Marylou Athanase[3,*], Antonio Sánchez Benítez[3], Tido Semmler[3]

[1] Department of Geography, University of California, Los Angeles, USA
[2]Nationalt Center for Klimaforskning, Danish Meteorological Institute, Copenhagen, Denmark
[3]Alfred Wegener Institute, Helmholtz-Centre for Polar and Marine Research, Bremerhaven, Germany

*marylou.athanase@awi.de

https://doi.org/10.5194/egusphere-2024-2214
Preprint. Discussion started: 4 September 2024

Abstract

The Arctic sea-ice cover and thickness have rapidly declined in the recent past. Snow cover on sea ice, acting as an insulating barrier, was shown to be instrumental in driving the variability and trends in sea-ice thickness. Because of this, the ability of climate models to realistically simulate the present-day annual cycles of Arctic sea-ice properties has become a central measure of model performance in Arctic-focused climate model intercomparisons. However, evaluating free-running model simulations usually requires multi-year observational datasets, which is challenged by the relatively short-term existing Arctic measurements particularly sea-ice and snow thickness. In this exploratory study, we propose a new methodology to improve the meaningfulness of sea ice and snow comparisons to model data. We make use of the exceptional year-long MOSAiC observations to examine the simulated Arctic sea-ice and snow thickness in 10 CMIP6 models. To perform meaningful comparisons with the modeled simulations, we define two "proxy years" selection methods based on sea-ice area and atmospheric criteria, when these conditions in the Arctic are similar to those during the MOSAiC year. We verify the capability of the proxy-year composites to capture the atmospheric and sea-ice variability, by comparing them with the sets of nudged simulations in which the atmospheric circulation observed during the MOSAiC year is directly imposed. Our results show that models tend to simulate similar annual cycles compared to the observations however, with an overestimation in amplitude for snow thickness and a misaligned phase of sea-ice thickness cycles. Overall, the study highlights that regardless of the specific modeled configurations and conditions within individual proxy years, biases in sea-ice and snow thickness remain consistent, even when wind conditions are imposed in the nudged model simulations. This highlights the necessity for a better representation of modeled processes driving the sea-ice and snow thicknesses which will be instrumental in the next generation of GCMs. This first MOSAiC-based assessment of the modeled snow and ice thickness, and the proposed proxy-year-based methodology, pave the way for further meaningful model evaluation.

https://doi.org/10.5194/egusphere-2024-2214
Preprint. Discussion started: 4 September 2024

1. Introduction:

Arctic sea ice, and especially the snow cover on top of it, plays a crucial role in the Arctic climate system due to its thermal properties as insulator and as reflector of incoming solar radiation. The Arctic sea ice has been declining rapidly over the recent decades which has major impacts on the Arctic climate system, on the global atmosphere and ocean circulation, and on biology (e.g. Hezel et al., 2012). Therefore, it is crucial to continuously observe changes in the Arctic sea ice and snow cover as well as to simulate those changes in a realistic way.

Previous studies have recognized several large-scale internal climate variability modes influencing Arctic sea ice changes. The Arctic Oscillation (AO) induces large-scale fluctuations in sea level pressure between the Arctic and mid-latitudes (Thompson and Wallace 1998). AO-related winds impact sea ice motion and export with seasonal lags (Rigor et al 2002, Ogi et al 2010). Other influential modes include the Quasi-Biennial Oscillation (QBO) in stratospheric winds and El Niño-Southern Oscillation (ENSO) linked to equatorial Pacific Ocean temperature fluctuations (Hu et al 2016). Additionally, the multidecadal Atlantic Multidecadal Oscillation (AMO) and Pacific Decadal Oscillation (PDO) affect Arctic sea ice trends (Day et al 2012). Among other factors, sub-mesoscale (Manucharyan et al., 2017) and mesoscale (Gupta et al., 2020) eddy fields rub against ice at the surface and through Ekman-induced vertical motion can bring warm waters up to the surface and partially melt the ice. Intense winter storms in the Atlantic sector of the Arctic can fracture the sea ice cover, intensify ocean-ice-atmosphere heat exchanges, and render the ice more susceptible to lateral melting (Graham et al., 2019). Anomalous atmospheric flows of warm and humid air into the Arctic region can further exacerbate these melt processes (Svensson et al., 2023).

Several studies have investigated Global climate models (GCMs), particularly CMIP6 models' capability to simulate sea ice and snow on the Arctic-wide basin scales, evaluating their performance in capturing snow and ice seasonality and overall volume distribution (Notz & SIMIP 2020, Zhou et al., 2021, Xu and Li 2023, Watts et al. 2021). The studies evaluating sea ice thickness (SIT) conclude that the overall seasonality and trends in simulated SIT agrees well with reanalysis and satellite derived SIT products, however large regional biases continue to exist (Xu and Li 2023, Watts et al. 2021). Arctic snow thickness over sea ice has not been assessed as thoroughly as the SIT, probably due to the fact that Arctic wide snow products over sea ice have only recently become available (Zhou et al., 2021). To our knowledge, Chen et al., 2021 is the only study which evaluates basin-wide snow volume from CMIP6 models against observation-based snow thickness products. They compared a passive microwave-based snow thickness product with the CMIP6 multi-model mean of snow volume and found that most models simulate a delayed snow maximum and an overall thinner snow than the satellite-based comparison products.

https://doi.org/10.5194/egusphere-2024-2214
Preprint. Discussion started: 4 September 2024

GCMs in general, usually suffer from very simplified sea ice and snow on sea ice parameterizations, and often only consist of one layer for sea ice and one layer for snow with a constant snow density (e.g. Webster et al., 2021; Blanchard-Wrigglesworth et al., 2015; Hezel et al., 2012). Depending on the model, strong positive or negative biases have been found and simulated snow thickness trends greatly differ between models (Webster et al., 2021). To better understand the biases identified in the above studies, more detailed observational studies are needed. Observation-based approaches to assess sea ice/snow and its variability have been quite limited, especially in the wintertime, due to the harsh conditions. Efforts have been made to use Operation IceBridge observations (MacGregor et al., 2021) combined with reanalysis data to reconstruct snow on Arctic sea ice (Blanchard-Wrigglesworth et al., 2018). However, existing observations suffer from strong spatio-temporal heterogeneities in the snow cover both in the thickness and in the density and/or the water content (e.g. Webster et al., 2018) that affect the thermal properties of the ice and snowpack. Therefore, high-quality sea ice and snow observations are essential to adequately sample the heterogeneities in the sea ice and snow cover for a thorough evaluation and subsequent improvement of GCMs.

An unprecedented effort has been made in the year-long MOSAiC expedition (October 2019 - September 2020) to sample an annual cycle of simultaneous observations in the ocean, atmosphere, ice and snow, including throughout the Arctic winter season (Rabe et al., 2022, 2024; Shupe et al., 2022; Nicolaus et al., 2022; Macfarlane et al., 2023). The research vessel Polarstern (Alfred-Wegener-Institut, 2017) was frozen in the Arctic sea ice and left drifting on an ice flow. Extensive measurements have been made in the surroundings of the research vessel (for snow and sea ice; see Nicolaus et al., 2022, Wagner et al., 2022), providing a unique dataset of year-long sea ice and snow-thickness data distributed over the size of a typical GCM grid cell. The snow thickness is especially valuable as this is difficult to retrieve from satellite data unless one has reliable reference observation data or uses a triple collocation method (He et al., 2023). There remain certain challenges in using the MOSAiC-derived SIT and snow data for a comparison with coarse resolution GCM simulations:

1. The spatial difference between measurements of sea ice and snow and their representation in GCMs (a point value in the former while averaged values at grid cell resolution in the latter).
2. The fact that the MOSAiC ice flow is drifting in space during the year.
3. The MOSAiC year is one realization of natural variability; while freely running climate models are not designed to simulate the characteristics of a specific year (e.g. atmosphere and ocean circulation that may lead to certain sea ice and snow patterns).

https://doi.org/10.5194/egusphere-2024-2214
Preprint. Discussion started: 4 September 2024

In this methodology-oriented study, we aim to address the above challenges by proposing a simple approach to perform meaningful comparisons of CMIP6 models with the field observations. We propose two proxy-year selection methods based on sea-ice area (SIA) and via atmospheric criteria (using AO) for a comparison of MOSAiC dataset with the *historical* experiments in 10 CMIP6 climate models. Furthermore, we perform another set of comparisons using nudging atmospheric circulations in a GCM during the MOSAiC year. We have divided this paper into five sections: In Sect. 2, we describe the observation and model data sets. Sect. 3 details the proposed observation - model comparison methods. Results of the comparison are given in Sect. 4 while Sect. 5 discusses the proposed methods and results and finishes with concluding remarks and ways forward. An overall understanding of Arctic sea-ice-snow simulation in coupled climate models including detailed analysis and explanation of specific critical processes affecting sea ice and snow thickness remains outside the scope of our study.

2. Datasets:

2.1. Observations

Our study utilizes observational datasets from the Ocean and Sea-Ice Satellite Application Facility (OSI-SAF) in the European Organization for the Exploitation of Meteorological Satellites (EUMETSAT) (Lavergne et al., 2019) for observed SIA over the pan-Arctic covering the time-period from 1979 to 2015. We further use the observed AO Index from NOAA's Climate Prediction Center (https://www.cpc.ncep.noaa.gov/products/precip/CWlink/daily_ao_index/ao.shtml) (Sect. 3.1.2).

Snow thickness in-situ observations from the MOSAiC drift, used in the model-observation comparison, have been collected by Sonar Snow Buoys (Nicolaus et al. 2021b) and by Sea Ice Mass Balance Buoys (IMB) (Lei et al. 2021). In-situ observations for SIT are only from IMBs. In total 32 buoys were considered in this study, which were deployed throughout the year in a 40 km radius around the MOSAiC ice floe (Nicolaus et al. 2022).

The Snow Buoys measure surface elevation change from the day of deployment. The distance is measured by four ultrasonic sensors mounted on a square rick on top of a 2.55 m pole. The snow thickness is derived from in situ snow thickness measurements at deployment and the measured elevation change. In addition to the elevation changes, the buoy also measures temperature and barometric pressure (Nicolaus et al. 2021b). In this study the preprocessed data set from Nicolaus et al. (2021a) was used. In the preprocessing all obvious inconsistencies were removed, and the resulting data comes,

https://doi.org/10.5194/egusphere-2024-2214
Preprint. Discussion started: 4 September 2024

where available, in 1-h intervals. The Snow Buoys are indicated by red markers in Fig.1 and are partly covered by the IMB buoys displayed in blue.

The IMBs measure snow and SIT taking advantage of their different thermal properties. To measure the SIT an array of heating elements and temperature sensors is suspended from the top of the snowpack to the ocean. Through cycles of heating and measuring the thermal diffusivity the surrounding medium can be determined to be ice, ocean, air or snow (Jackson et al. 2013). This allows for a simultaneous measurement of both ice and snow thickness. The data used in this study was processed by Lei et al. 2021. The IMBs measure at a frequency of 1 day and have an accuracy of 0.02 m.

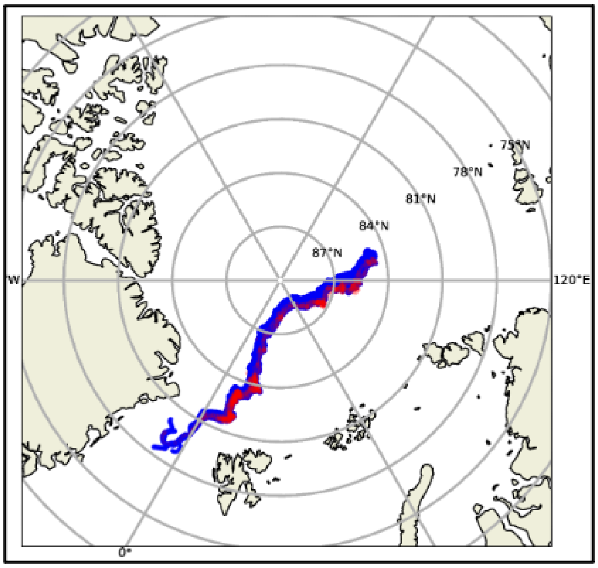

Figure 1: Location of our study area. This corresponds to the trajectory followed in the MOSAiC expedition (September 2019 to August 2020). The Snow Buoys and IMB Buoys are indicated by red and blue markers respectively.

2.2 CMIP6 Models

We analyze the monthly averaged variables over the sub-period 1979-2014 within the *historical* experiments of 10 CMIP6 models (Eyring et al., 2016; Notz et al., 2016) (Table 1). We focus on the *"sithick"* variable, representing simulated effective floe thickness. We also incorporate *"siconc" viz.* sea-ice concentration and *"sisdthick"* representing the snow thickness. The SIT values used throughout the study for all the climate models, are weighted by the *"siconc"*. Additionally, for the proxy year selection, we use the variables- "*siarean*" and "*zg*" at 1000 hPa, representing the cumulative SIA over the Northern Hemisphere and the geopotential height, respectively. To not give extra weight to models

https://doi.org/10.5194/egusphere-2024-2214
Preprint. Discussion started: 4 September 2024

providing multiple ensemble members, and for consistency with previous CMIP6 based sea-ice comparison studies (SIMIP Community, 2020 and Roach et al., 2020), we considered the first ensemble member for each selected model (Table 1). This exploratory study tests our proposed methodology on 10 CMIP6 models and a single ensemble. For NorESM2-MM, we have utilized the SSP585 scenario for selecting proxy years according to the SIA based criterion (Fig.5) as its *historical* values did not reach observed sea ice characteristics during the historical period but only during the future scenarios (not shown) (Seland et al., 2020).

Table 1: Details of the specifications of 10 CMIP6 models used in the study.

Model Name	**Atmospheric Model**	**Ocean Model**	**Sea-Ice Model**	**References**
AWI-CM-1-1-MR	ECHAM6.3.04p1 [100km]	FESOM 1.4 [25km]	FESIM 1.4 [25km]	Semmler et al., 2018
CESM2	CAM6 [100km]	POP2 [100km]	CICE5.1 [100km]	Danabasoglu et al., 2019
CESM2-FV2	CAM6 [250km]	POP2 [100km]	CICE5.1 [100km]	Danabasoglu et al., 2019
CESM2-WACCM-FV2	WACCM6 [250km]	MAM4 [100km]	CICE5.1 [100km]	Danabasoglu et al., 2019
CESM2-WACCM	WACCM6 [100km]	MAM4 [100km]	CICE5.1 [100km]	Danabasoglu et al., 2019
MPI-ESM-1-2-HAM	ECHAM6.3 [250km]	MPIOM1.63 [250km]	UNNAMED (thermodynamic (Semtner zero-layer) dynamic (Hibler 79) [250km]	Neubauer et al., 2019
MPI-ESM1-2-HR	ECHAM6.3 [100km]	MPIOM1.63 [50km]	UNNAMED (thermodynamic (Semtner zero-layer) dynamic (Hibler 79) [50km]	von Storch et al., 2019
MPI-ESM1-2-LR	ECHAM6.3 [250km]	MPIOM1.63 [250km]	UNNAMED (thermodynamic (Semtner zero-layer) dynamic (Hibler 79) [250km]	Wieners et al., 2019
NorESM2-LM	CAM-OSLO [250km]	MICOM [100km]	CICE [100km]	Seland et al., 2019
NorESM2-MM	CAM-OSLO [100km]	MICOM [100km]	CICE [100km]	Bentsen el al., 2019

https://doi.org/10.5194/egusphere-2024-2214
Preprint. Discussion started: 4 September 2024

2.3 Nudged simulations

We perform nudged simulations, in which the wind evolution observed before and during the MOSAiC year is imposed in coupled climate models. In this study, we employ the nudged simulations to determine whether the atmospheric flow is the dominant driver of the MOSAIC-year snow and ice variations. Additionally, we use the nudged simulations to test the skill of the proxy-year selection criteria: we compare the annual cycles of sea-ice and snow thickness obtained using the nudged simulations and using the proxy-year selection criteria. This reveals whether model-observations discrepancies arise from a mismatch in anomalous weather conditions, or from insufficient process representations.

Our nudged simulations are based on two coupled climate models with spectral nudging capabilities, the AWI-CM-1 (Sidorenko et al., 2015; Rackow et al., 2018) and AWI-CM-3 (Streffing et al., 2022) developed at the Alfred Wegener Institute. The AWI-CM-1 model is composed of ECHAM6.3.04p1 from MPI-M (Stevens et al., 2013) for the atmosphere component, and FESOM1.4 (Wang et al., 2014) for the ocean and sea ice component; henceforth called ECHAM6/FESOM. As introduced in the previous section, free-running simulations from ECHAM6/FESOM contributed to CMIP6 (Semmler et al., 2020). In the more recently developed AWI-CM-3, the atmosphere model OpenIFS 43r3 (ECMWF, 2017) is coupled to the ocean and sea ice model FESOM2 (Danilov et al., 2017; Danilov et al., 2015), therefore we henceforth refer to this model as OpenIFS/FESOM2.

In the nudged simulations, we directly impose, via spectral nudging, the evolution of the atmospheric circulation, characterized by the vorticity and divergence, as observed during the MOSAIC year (until August 2020) using ERA5 data, with a relaxation timescale 1h and a spectral truncation 20 (on zonal wavenumbers for ECHAM6/FESOM, on all wavenumbers for OpenIFS/FESOM2) (Sanchez-Benitez et al., 2022; Pithan et al., 2023). Only vertical levels between 700 hPa and 100 hPa are nudged, leaving the atmospheric boundary layer and the stratosphere, and all other physical parameters (e.g., temperature, surface pressure, humidity, clouds, precipitation, and sea-ice) to evolve freely according to the models' physics. For both models, three ensemble members are nudged from the 1st of January 2017 onwards, initialized from CMIP-type historical and subsequent ssp370 scenario forcing simulations. Note that while ECHAM6/FESOM contributed to CMIP6, OpenIFS/FESOM2 is a prototype post-CMIP6 model and therefore is not included in the models used for proxy-years selection.

3. Methods:

This exploratory study attempts to make a step forward in assessing the ability of state-of-the-art global climate models from CMIP6 (Coupled Model Intercomparison Project 6:

https://doi.org/10.5194/egusphere-2024-2214
Preprint. Discussion started: 4 September 2024

Eyring et al., 2016) to simulate the annual cycle of observed sea-ice and snow thickness. To address the three challenges mentioned in Sect. 1, we applied following solutions:

- Model-observation spatial scale discrepancies were tackled by averaging over a large number of snow and SIT autonomous buoy observations recorded during MOSAiC. Since GCMs provide a single mean value of SIT and snow thickness for each grid cell, they are assumed to represent the average SIT over the entire area covered by the GCMs' grid. In reality, SIT and snow cover can vary greatly within a typical area of one GCM grid cell (Nicolaus et al. 2022), therefore, averaging over a large number of observations contributes towards making it comparable.
- To address the flow drift, we collocate the model values with observations per day (in the daily nudged runs) or month (in monthly CMIP6 runs).
- To address the CMIP6 models' inability to simulate specific years, we propose three methods to enable meaningful year-to-year comparisons : (i) a simple proxy year approach using the simulated sea ice area (SIA) (ii) another proxy year selection using atmospheric criteria (AO); and (iii) a nudging approach in which the atmospheric circulation of the GCM is relaxed towards the observed winds in the mid-troposphere.

3.1. Selection of proxy years

In the CMIP6 models, proxy years were chosen to align the simulated fields with the sea-ice and atmospheric conditions experienced during the MOSAiC measurement period. To ensure a thorough evaluation, we employed two distinct selection criteria: one based on sea-ice conditions and the other on atmospheric circulations observed during the MOSAiC study period. Ocean currents and heat transports are also important contributors in decreasing the Arctic sea-ice area and volume; however, contributions from the oceans in driving sea-ice loss are still uncertain (Docquier et al., 2021). This study does not cover the role of oceans in influencing sea-ice simulations in the models.

For an accurate and comprehensive selection of proxy years with characteristics similar to the MOSAiC year, it is crucial to eliminate divergences from observations which arise from the free-running models' different realizations of natural variability. Therefore, our method refines the selection process by excluding conditions (or years) vastly different from those observed during MOSAiC, ensuring the chosen years mirror the sea-ice and atmospheric conditions of the study period. This nuanced approach illuminates the complex dynamics shaping these simulations, empowering us to make informed decisions about proxy year representation.

https://doi.org/10.5194/egusphere-2024-2214
Preprint. Discussion started: 4 September 2024

3.1.1. Proxy Years based on sea-ice conditions:

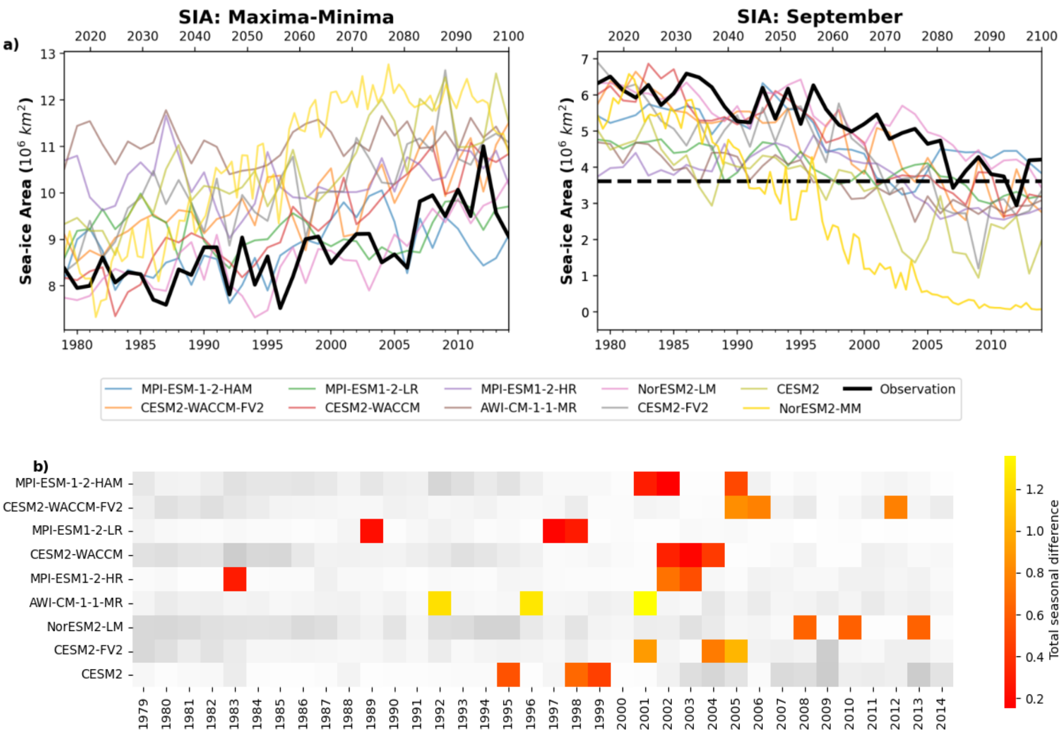

Figure 2: a) Selection of sea-ice based proxy years. Colored lines represent the SIA values for different CMIP6 models while the solid black line represents observations (OSI-SAF). Black dashed line corresponds to the observed mean SIA value for the MOSAiC year. Secondary x-axis corresponds to the SSP585 scenario selected for the NorESM2-MM (Gold line). **b)** Heatmap showing the seasonal differences between each year in the *historical* CMIP6 models and the SIA values for the MOSAiC year. Highlighted are the three proxy years with lowest three differences, selected for each model between 1979-2014 based on their proximity to the annual SIA values.

We selected SIA as a criterion for our proxy year selection instead of SIT due to the limited availability of Arctic-wide SIT observation data, which primarily relies on radar and laser altimetry-derived satellite freeboard data. This has high uncertainty due to overlying snow and inaccurate snow-ice interface (Willatt et al., 2010). Using SIA datasets allows us to identify similar Arctic-wide conditions and ensures that models remain consistent with observed sea-ice extent during the MOSAiC period.

The selection of sea-ice based proxy years was conducted using two key indicators: Firstly, we considered the difference between the maximum (March) and minimum (September) SIA which served as an estimate of the first-year ice component. Secondly, we examined the SIA during the minimum period (September) to estimate the contribution of multi-year ice during those years. We selected three proxy years that satisfied both the

https://doi.org/10.5194/egusphere-2024-2214
Preprint. Discussion started: 4 September 2024

criteria implying that their SIA values were the closest to the observed values during the MOSAiC year (Fig.2). By concentrating on these specific proxy years, we aimed to replicate the contributions of both the first-year and multi-year ice in shaping the sea-ice and snow distributions in a particular year.

3.1.2. Proxy Years based on atmospheric (circulation) conditions:

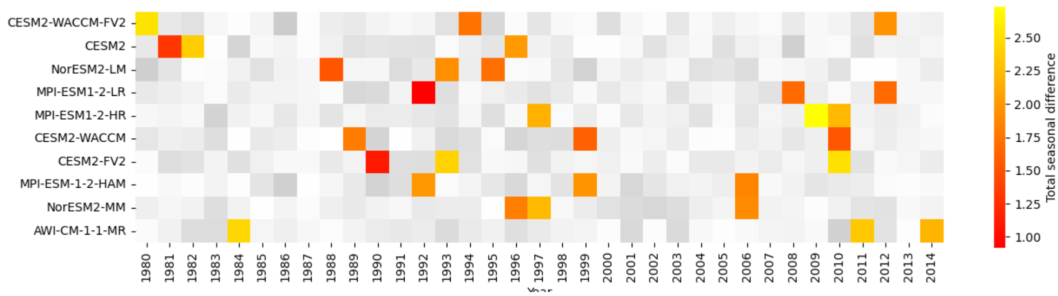

Figure 3: Atmospheric circulation-based proxy years. Heatmap showing the seasonal differences between each year in the *historical* CMIP6 models and the AO values for the MOSAiC year. Highlighted are the three proxy years with lowest three differences selected for each model between 1979-2014 based on their proximity to the seasonal AO values.

The AO refers to an atmospheric circulation pattern over the mid-to-high latitudes of the Northern Hemisphere. AO is the dominant mode in the central Arctic (Thompson & Wallace, 1998) playing a major role in shaping the sea-ice/snow distributions (Wang & Ikeda, 2000). The most obvious reflection of the phase of this oscillation is the north-to-south location of the storm-steering, mid-latitude jet stream. Thus, the AO can have a strong influence on weather, climate, and the sea-ice variability in the high- to mid-latitude Northern Hemisphere. During the MOSAIC year, the AO experienced large shifts, ranging from a highly negative index in November 2019 to an extremely positive index during January–to–March 2020, marking it as an anomalous year in AO behavior (Dethloff et al., 2022).

Given this context, our evaluation considered the proximity of the seasonal AO values in climate models to the corresponding values observed during the MOSAiC year. Specifically, we compared the simulated AO values during the winter season (January–to–March) of a given year and the November values in the preceding year. For each CMIP6 model, we identified three years in the *historical* period which exhibited the smallest differences from the observed seasonal AO indices (capturing extreme AO trends during both winter and November) (Fig.3). The selected proxy years are presumed to replicate the anomalous atmospheric conditions prevalent during the MOSAiC year. This methodology thus involves comparing AO values in corresponding periods and

https://doi.org/10.5194/egusphere-2024-2214
Preprint. Discussion started: 4 September 2024

selecting proxy years based on minimizing differences, thereby ensuring a close alignment with the observed AO dynamics.

3.2. Colocation to MOSAIC drift trajectory

In this study, the selection of grid cells in the climate models was based on the MOSAiC trajectory. This collocation was done by determining the maximum north, south, west, and east extent of active snow and ice buys within one day/month and selecting the model grid cells covering this extent. However, it is important to note that due to the varying resolutions and projections of the original grids used in the CMIP6 models, we selected a different number of total grid cells per month and model. The modeled area in different months across selected CMIP6 models following the MOSAiC trajectory shows the grid areas ranging from a maximum of 3579 km^2 (for MPI-ESM-1-2-LR in the month of November) and the minimum of 999 km^2 (for the CESM2-versions in the month of July) during the MOSAiC year. In comparison, the distributed network of MOSAIC spanned a 40 km radius. Instruments used in this study drifted throughout the year but remained within a ~30 km radius, that is, within an area on the order of 2000-3000 km^2 assuming a roughly circular distribution (Rabe et al., 2024). This is thus on the same order of magnitude as the colocated model cells. Our study, therefore, accounts for variations in location and covered area to accurately interpret the modeled data and draw meaningful conclusions (Sect. 3.3).

Following the selection of the three proxy years, we conducted a comprehensive assessment of the annual cycles averaged over the MOSAiC flow trajectory. This evaluation served as a critical step in our research, enabling us to investigate the temporal variability in the Arctic floe and snow thickness simulations and compare them with the in-situ observation dataset. By employing these data and methods, we have established an initial step towards comparing the in-situ measurement campaign sea-ice and snow thicknesses in the GCMs in the Arctic.

3.3 Processing of snow and ice observations

The Snow Buoys and SIMBA buoys measure at different frequencies and resolutions. To get a thickness estimate comparable to model grid cell values, each active buoy was averaged to a daily value. From this the mean snow and SIT was calculated, shown in black in Fig. 4a and b. From all buoys that are part of this averaging per day the most northern, southern, western, and eastern location was determined to estimate the area over which the buoys were averaged. Fig.4c shows the number of active buoys per day. Overall, there were 13 Snow Buoys and 19 IMB buoys active throughout the period. The

https://doi.org/10.5194/egusphere-2024-2214
Preprint. Discussion started: 4 September 2024

maximum number of instruments measuring snow thickness for one day was 23, while for SIT it was 17.

The monthly mean was calculated from the daily averaged values in Fig.4. The locations for the model comparison were selected similarly as the locations for the daily mean, by selecting the maximal east-west and north south coverage of all observations considered within one month.

3.4 Methodology Validation using Monte Carlo Method

Our research methodology integrated the Monte Carlo Method (Sect. 4.3) with a robust proxy year selection process (described in Sect. 3.1) to assure the reliability of our two methods (which are physical selections) by comparing them with the random selections. We utilized the 10 selected *historical* CMIP6 model simulations (same as described in Sect. 2.2), for the period 1979 to 2014. We applied the resampling technique known as bootstrap, which randomly selected three years during each of the 10,000 iterations for all the selected models. This process generated a multitude of random possible combinations, encompassing various annual cycles for SIT and Snow Thickness. This approach served as a *validation* to investigate if our proxy year selection methods gave added value compared to randomly selected years.

4. **Results**

4.1 Comparisons for different In-situ observations

To bridge the gap between model resolution and point observations a multitude of observations from the MOSAiC campaign were considered to evaluate the GCMs snow and ice thickness. The snow thickness observations considered are shown in Fig.4a. Both Snow Buoys and IMBs were considered in the average, which is calculated as the mean between the IMB and Snow Buoy measurements, weighted by the number of active buoys per day shown in Fig.4c. The IMB snow and ice numbers of observations in Fig.4c differ in summer 2020, because negative snow measurements are excluded. The Snow Buoys measurements showed an overall lower snow thickness than the IMB buoys for most of the winter. From November to February, the snow buoys measured a slight decrease in snow thickness, while the IMB buoy measured a slight increase. This could be due to a relatively high drop in active sensors in January/February 2020 for the Snow Buoys, as shown by the red line in Fig.4c.

https://doi.org/10.5194/egusphere-2024-2214
Preprint. Discussion started: 4 September 2024

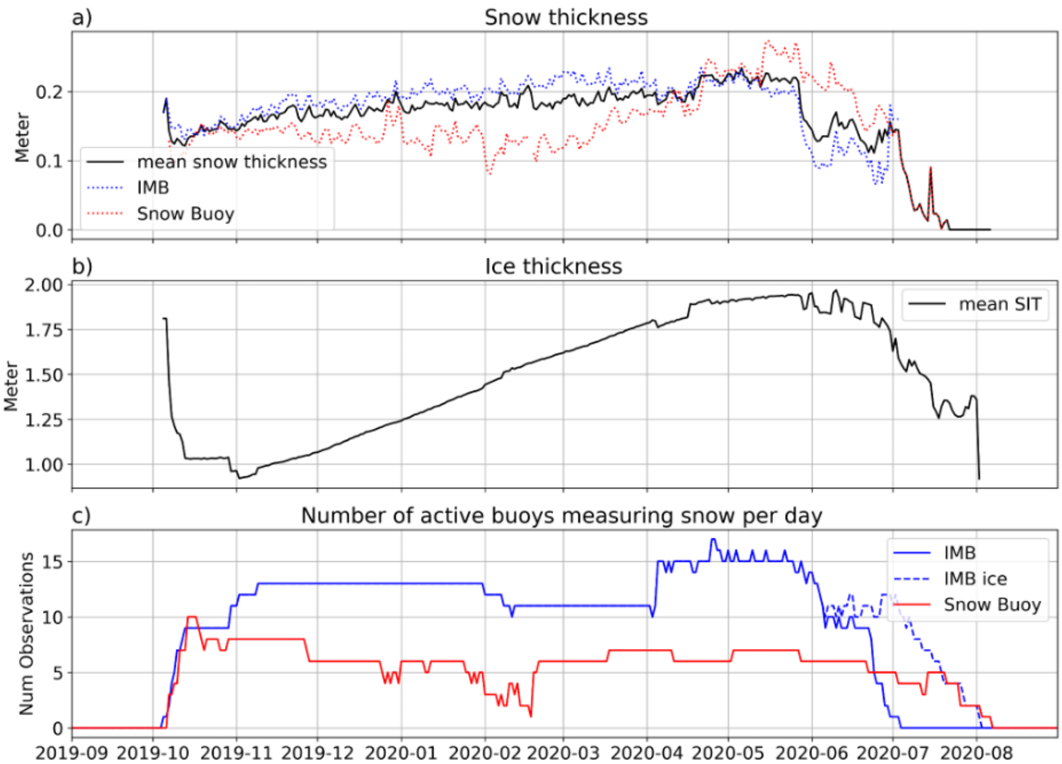

Figure 4: Time series of sea-ice and snow parameters along the MOSAIC drift track. (a) Snow thickness (m) and (b) sea ice thickness (m) (c) Number of active buoys. IMBs measure sea ice and snow thickness, Snow Buoys measure solely the snow thickness.

The SIT observations considered are shown in Fig.4b. There are less daily SIT observations than snow observations because the Snow Buoys only measure snow thickness, so only the IMBs are considered. In the very beginning and end of the observation period, there are large variations in the mean SIT which result from a fewer number of active buoys. One IMB buoy measuring about 1.8 m SIT from the beginning of October is causing the thick sea ice observations in the beginning of the observation period. This buoy is continuously measuring thick sea ice, but as the number of observations displayed in Fig.4c rises, the anomalous thick observation loses influence in the mean. Consequently, this increase in the number of measurements causes an apparent decrease in SIT from October to November in the monthly mean observed SIT (Figures 5a, 6a and 8a). As both platforms require sufficient SIT to be deployed, thin and fragile SIT conditions are thus under-documented in their measurements. This must be kept in mind when comparing the observations to the model values, mainly in early autumn or summer.

https://doi.org/10.5194/egusphere-2024-2214
Preprint. Discussion started: 4 September 2024

4.2 Reproduction of Annual Cycles for sea-ice variables:

4.2.1 Variations in Sea-ice thickness :

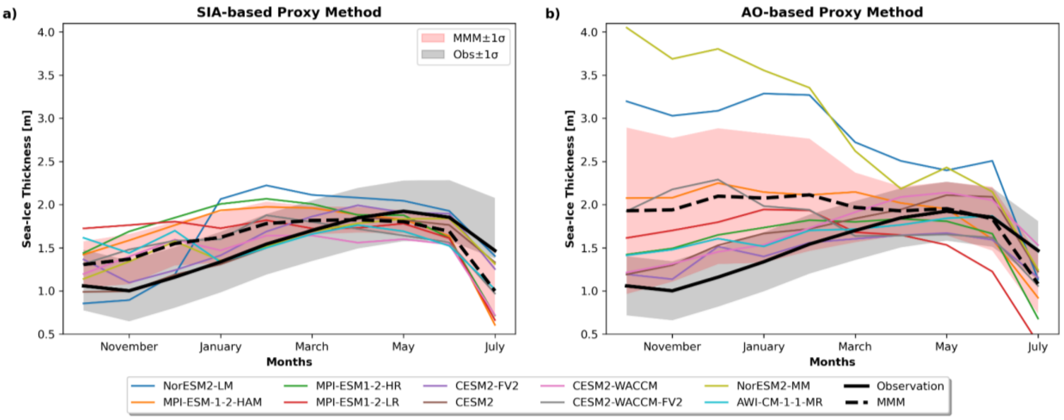

Figure 5: Annual cycles for SIT averaged over the three selected years from (a) SIA-based and (b) AO-based methods. The parameters are averaged along the MOSAiC trajectory. The black solid line corresponds to the in-situ observations and black dashed shows the Multi-model Means (MMM). The colored lines represent different CMIP6 models. The shaded red areas represent +-1 Standard Deviation for the MMM, and the gray shaded areas represent +-1 Standard Deviation for the observations.

In this section, we examine the capability of CMIP6 models to capture the SIT annual cycles during the MOSAIC year, using proxy years based on the SIA as well as atmospheric or AO-based criteria. Our observational SIT data reveals a consistent rise from November to May, followed by a decline. This aligns with the findings using PIOMAS (Chen et al., 2023), highlighting a peak SIT in May. However, when employing SIA-based proxy years, CMIP6 models tend to exhibit positive biases during cooler seasons (Fall and Winter) in SIT, followed by underestimations in warmer periods (Spring and Summer) (Fig.5a). Some models even indicate an early SIT peak between January and March. This is because the modeled sea-ice averages build up too quickly in winter and spring and then melt too rapidly in late spring, as noted by Webster et al., 2021. Consequently, the multi-model mean (MMM) shows nearly constant SIT values between February (peak) and June.

Fig.5b shows the annual cycles of SIT derived from monthly means of three proxy years determined using the AO criterion. *Firstly*, in comparison to the SIA-based proxy years, the inter-model spreads remain relatively higher for SIT particularly during the cooler seasons of Fall and Winter. *Secondly*, there are also higher biases evident in the models when compared to the SIA-based proxy years primarily during winters, while maintaining simulations of thinner sea-ice for the remainder of the year. These exaggerations in the MMM are caused mainly due to the influence of NorESM2-models. NorESM2-MM displays substantial positive biases between October-April when compared with the

https://doi.org/10.5194/egusphere-2024-2214
Preprint. Discussion started: 4 September 2024

observations as well as its values selected in Fig.5a. These overestimations can be anticipated to the characteristics of this model making it colder in the Arctic than its lower resolution counterpart– NorESM2-LM, hence thicker sea-ice in the Arctic Ocean (Seland et al., 2020). Additionally, when compared to the SIA criteria, the considerably thicker SIT values as well as the earlier peak observed in the NorESM2-MM for the AO criteria may arise due to the use of different scenarios.

The inter-model spread between all the models is often used as the metric to quantify the uncertainty in model simulations. Here, the model spreads for SIT are relatively higher during the late fall and winter seasons but begin to decrease starting in March. By May to July, the models exhibit a high degree of agreement in both methods. This result is in line with the previous studies conducted for the sea-ice extent in the Arctic (Shen et al., 2021). The inter-model spread of annual mean in SIT is 0.23- and 0.57-meters using SIA- and AO-based criteria respectively (Fig.5).

Overall, when compared to the observations, the models struggle to accurately capture the annual cycle of SIT using both the criteria. Both methods highlight an overestimation of SIT in Autumn and Winter, and an underestimation in Spring and Summer. Despite such biases and inter-model spreads, the overall patterns in the annual cycles of SIT look very similar across both the proxy-year selection criteria. Both the proxy year selection methods manage to capture annual cycles, albeit at different points in the year.

4.2.2. Variations in Snow Thickness:

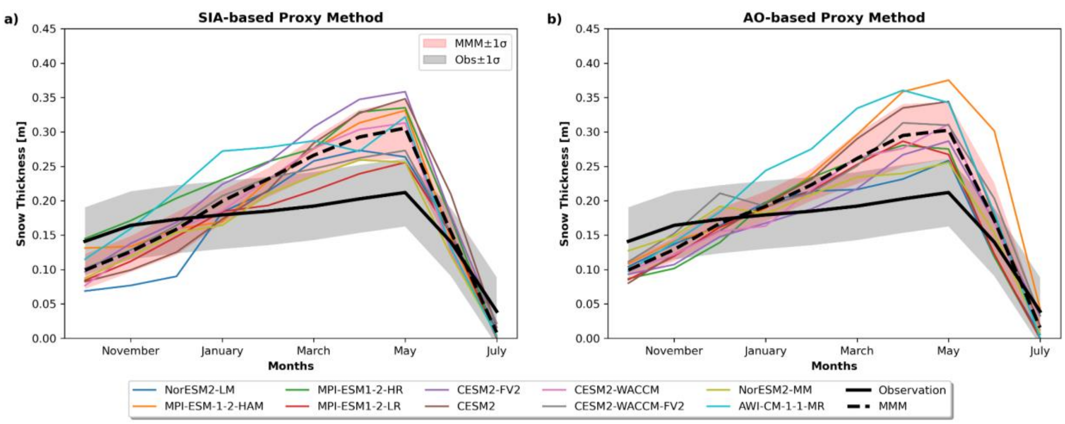

Figure 6: Same as Figure 5. Annual Cycles for Snow Thickness.

The snow thickness obtained with the SIA-based proxy-year selection criterion tends to be underestimated in all the models between October-January (Fig.6a). Snow thickness biases become progressively positive till May with notable improvement and

https://doi.org/10.5194/egusphere-2024-2214
Preprint. Discussion started: 4 September 2024

synchronization with observations starting in June, when a strong decline both in observations and model is noticed. For the snow thickness, the patterns and biases are similar across both the proxy methods with greater alignment compared to the SIT cycles. Particularly for the AO-based proxy method, we find very low values for snow thickness in October and November which significantly increase in Winter and Spring. Figures 6, 7 and 8 show that the snow growth is overestimated in climate models compared to observation, which could also explain the comparable lower SIT growth rate. Comparing the two methods, annual cycles of snow thickness obtained have similar intermodal spread of 0.03 meters. However there does exist a slightly higher disagreement between models using the AO-based proxy method particularly between March-June with relatively greater agreements at the start and the end of the cycles. In summary, annual cycles of snow thickness show maximum alignment during early Summer and Fall across both the proxy-year selection methods.

4.3 Nudged simulations for the MOSAiC period

We use nudged coupled simulations, in which the winds observed during MOSAIC are imposed (see Sect. 2.3), to examine whether discrepancies in the proxy-based ice and snow cycles arise from mismatching weather conditions or from insufficient process representations.

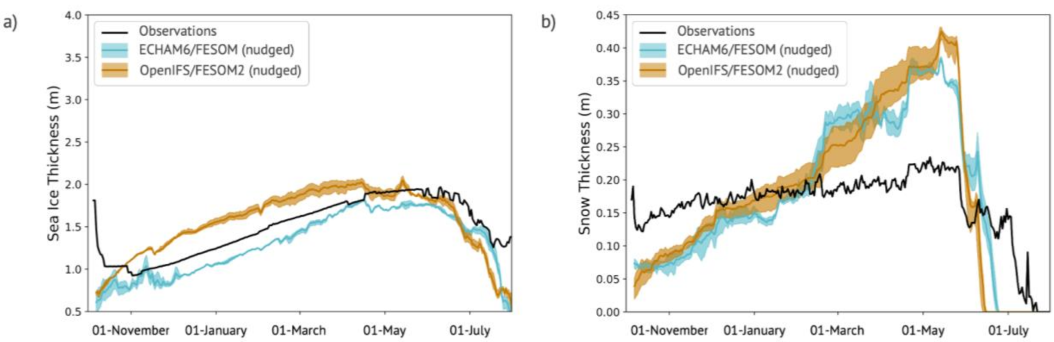

Figure 7: Annual cycles of sea-ice and snow parameters from the nudged simulations. (a) Daily SIT and (b) daily snow thickness along the MOSAiC trajectory; the black line represents in-situ observations, and rest show nudged simulations in which the evolution of winds observed during the MOSAIC year is imposed. Climate models used are ECHAM6/FESOM (blue) and OpenIFS/FESOM2 (orange). Shaded areas are the ensemble range for each set of coupled climate simulations, thick lines are the ensemble mean.

We find that the nudged simulations reproduce well the MOSAIC SIT annual cycle, despite a mild underestimation for ECHAM6/FESOM and overestimation for

https://doi.org/10.5194/egusphere-2024-2214
Preprint. Discussion started: 4 September 2024

OpenIFS/FESOM2 (Fig.7a). This indicates the importance of the atmospheric circulation in shaping the seasonal variations of SIT along the MOSAIC track. Both nudged simulations capture a more realistic SIT amplitude and seasonal signal than the AO-based proxy in Fig.6. The monthly AO index is thus likely insufficient to fully capture the evolution of the atmospheric circulation, and its influence on the SIT variations. In contrast, the SIA-based proxy demonstrates a comparable performance to the nudged simulations (compare Figures 5a and 7a). Indeed, the nudged simulations and SIA-based proxy exhibit a similar range in amplitude (from 0.8 to 2m). Both feature an annual SIT maximum in the late winter to spring, although it is slightly better captured in nudged simulations in April to June (Figures 5a and 7a).

In parallel, the snow thickness in nudged simulations exhibits a persisting too large annual cycle of snow accumulation, too little snow in the fall-winter and too thick snow in the spring (Fig.7b). The nudged simulations thus perform similarly to both SIA-based and AO-based proxies in representing the MOSAIC snow thickness annual variations (compare to Figures 5b and 6b). Yet, we note that precipitation and snowfall in nudged simulations follow closely the observations, with monthly accumulated values comparable to ERA5 within a 0.005 m difference (not shown). This confirms that biases in snow thickness accumulation is not primarily driven by the atmospheric flow, which is captured in the nudged runs, but rather by other processes of snow advection and melt insufficiently represented in CMIP6 and nudged models. We further discuss these processes in Sect. 5.

We thus conclude that on monthly to seasonal timescales, the SIA-based proxy year approach performs comparably as well as the nudged simulations approach. The nudged simulations nevertheless present a notable skill in capturing sea ice and snow variations on shorter, weekly to daily timescales. Indeed, despite their biases in amplitude, both nudged models reproduce several observed sudden changes likely linked to atmospheric conditions. For example, the drop in SIT in July, and peaks in snow thickness in late February, late April and mid-June, are well represented. Nudged simulations therefore have potential in supporting the analysis of short-lived events such as heavy snowfall, storms, or air intrusions, for which the proxy year criteria are limited.

4.4 Monte Carlo simulations for the annual cycles

Figure 8 illustrates the annual cycles of SIT and snow thickness, derived from a sample of 10,000 simulations using the Monte Carlo Method, with three years selected randomly. It shows that the variability in SIT modeled data is relatively high when compared to the snow thickness. However, this reduces for SIT starting May. Regarding the seasonal evolution of SIT, the MMMs derived from proxy years selected using the AO criteria lie close to the mean of the bootstrap distribution, pointing to a lack of performance of this

https://doi.org/10.5194/egusphere-2024-2214
Preprint. Discussion started: 4 September 2024

criterion to capture the conditions during the MOSAiC campaign as discussed before and improved by the use of nudged simulations. Meanwhile, with the SIA selection criterion, this is not the case, with the period October-February statistically different from the random distribution and not far from the “extreme limits” for the remaining months. It is worth pointing out the fact that the SIA-based proxy method produces extreme values closer to observations, indicating that it tends to select years with unusual or rare conditions, like the one associated with MOSAiC. This alignment with observations can be seen as a positive aspect, indicating that our method captures real-world scenarios, albeit rare ones. When comparing the MMMs from both the proxy-selection methods, starting in March, the methods align closely, with their values closely matching the observations.

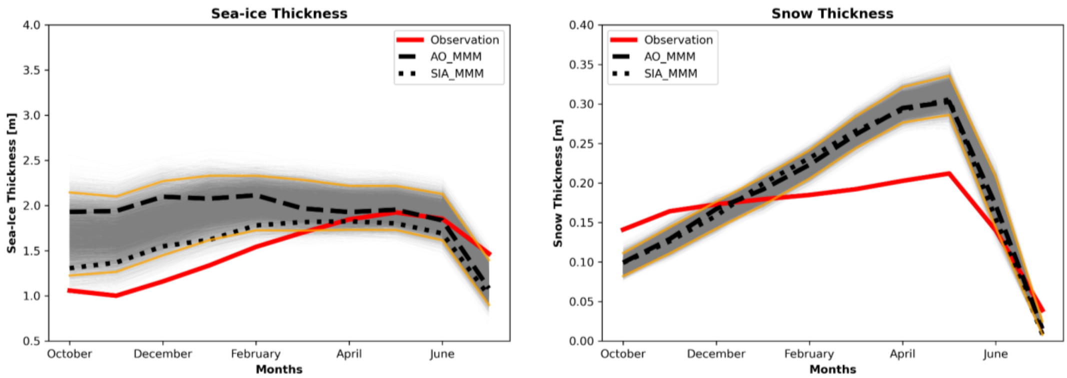

Figure 8: Annual cycles for MMMs of SIT and Snow Thickness using randomly selected years. The year selection is made using Monte Carlo Method which randomly selects three years over the contiguous chunk of 36 years (1979-2014) and the process is repeated 10,000 times. Each gray line represents MMM calculated over 10 models for 3 random years per iteration with 10,000 total iterations. The black dashed and dotted lines correspond to the MMM obtained by using the proxy years from AO and sea-ice criteria, respectively. The solid red lines represent in-situ observations. The orange lines correspond to the 2.5 and 97.5 quantiles for the MMM.

Turning to snow thickness, the models appear to struggle in replicating even a single year through bootstrapping that closely resembles the observed data, as they consistently show lower values in autumn and higher values in May. The AO and SIA-based proxy years, though exhibiting significant similarity throughout the year, do not perform better than the randomized distribution using the Monte Carlo Method. Notably, the randomized distribution never includes conditions approaching the observations during the MOSAIC year conditions. This suggests that, as seen in the nudged simulations as well, the model discrepancies in simulating snow thickness primarily stem from the inadequate representation of crucial processes, many of which are either underdeveloped or entirely absent in current coupled climate models.

https://doi.org/10.5194/egusphere-2024-2214
Preprint. Discussion started: 4 September 2024

5. Discussions

This study proposes a new proxy-year selection approach to perform meaningful comparisons of CMIP6 models' sea ice and snow data with measurements relatively localized in time and space – here, using the unique MOSAIC time-period and observations– tailored to a specific trajectory (and not circumpolar Arctic). We propose this method in an exploratory study using a first set of 10 selected CMIP6 models. We employ two proxy-year selection methods: one based on SIA and the other on atmospheric or AO, to select proxy years with sea-ice and atmospheric conditions similar to those observed during the MOSAiC year. Both methods account for the observed spatio-temporal variabilities in the specific criteria used, ensuring a closer approximation to the sea-ice and atmospheric conditions during the study period. The selected proxy years are then evaluated in light of atmospherically nudged simulations from two AOGCMs for the MOSAiC year, and finally validated using Monte Carlo Simulation where the significance of the annual cycles was tested over 10,000 random iterations. Our two proxy year selection methods demonstrate performance comparable to that of atmospherically nudged simulations, underscoring the robustness and usefulness of our methodology. This finding highlights the effectiveness of our experimental yet relatively simple approach in using the free-running CMIP6 models to achieve outcomes similar to the more precise and observationally constrained nudged simulations. Such methods are particularly valuable for institutions that lack the resources to produce their own nudged simulations, offering a viable alternative that maintains relatively better accuracy. Therefore, this study offers a particular methodology that can serve as one of the many comparison possibilities between coupled climate models and field observations.

Our results highlight biases and seasonal differences in the model simulations of both SIT and snow thickness along the MOSAiC drift. For the snow thickness, we find that models overestimate the amplitude of the annual cycle – with quite large, simulated accumulation and melt. To investigate possible reasons for overestimated snow accumulations, we compare snowfall in the nudged simulations and ERA-5, which highlighted a good agreement (not shown). Furthermore, Wagner et al. (2022) found that snowfall in ERA-5 during the MOSAiC expedition slightly exceeded their observations. This discrepancy was on a scale similar to what we observed in our comparison, suggesting that difference in snowfall cannot be the sole cause for the bias in snow thickness. Instead, other processes such as snow advection and melt, which are insufficiently represented in CMIP6 and nudged models may likely contribute to this bias (e.g., Chen et al., 2021, Nicolaus et al., 2022, Pithan et al., 2023). Other sources of overestimation could be related to processes of snow densification. Warren et al. 1999 showed that snow density increases throughout the winter season, causing its volume to decrease, a process not included in the ice models to our knowledge. However, accounting for the densification would likely not lead to a large enough volume decrease to explain the differences between models and

https://doi.org/10.5194/egusphere-2024-2214
Preprint. Discussion started: 4 September 2024

observation. Another process not included in at least 7 of the 10 models is snow reduction into leads, which might occur under certain atmospheric conditions and can reduce the snow thickness by up to 10% (Clemens-Sewall et al. 2023). Further, it should be noted that the observation stations need to be set up on level ice and that snow is redistributed towards ridges by wind (Sturm et al. 2002). This might lead to an anomalously thin observed snow layer, while coarser-scale model grids average the snow cover over both level and ridged ice.

From the overestimated snow thickness in March, all models progress to an underestimated snow thickness in July, with melt happening faster and at higher rates than observed. A study analyzing the mean Arctic-wide snow thickness came to similar conclusions (Chen et al. 2021), indicating that this is a general feature of CMIP6 models and not introduced by the comparison methods implemented in this study. The melt of snow on sea ice is mainly forced by the onset of incoming shortwave radiation, strongly governed by the albedo. Perovich et al. (2002) describes the albedo evolution of Arctic snow throughout the melt season. As melt progresses, they describe the albedo as a highly spatial variable, with a mean of 0.4, with individual values ranging between 0.1 and 0.65. The models are not capable of resolving such local processes at their resolutions. Furthermore, the albedo is often a parameter tuned to ensure correctly simulated sea ice extent (Hunke et al. 2010, Losch et al. 2010). In essence, our results show that the melt of snow is overestimated in the CMIP6 models, and the albedo would be a good starting point to investigate the origin of this overestimation.

Turning to SIT, our results show that models better reproduce variations in thickness between March and July compared to that between October and February when the biases and inter-model spreads are relatively higher. This difference in performance of CMIP6 models in the two periods may be due to regional or inter-annual differences caused by the proxy year selection, which may also impose a strong decadal trend amongst the individual years. Previous studies considering the Arctic-wide sea ice volume in CMIP6, such as Winkelbauer et al. (2024), do not show compatible patterns. The bias and model spread in Winkelbauer et al., (2024) are relatively consistent throughout the year. Our study differs from this previous work in terms of selection of specific proxy years and the unique MOSAiC trajectory for the comparison. Seasonal variations of biases and inter-model spread are present in both proxy year sections and the Monte-Carlo method, with the AO-based method showing the most pronounced variations. The seasonality of large inter-model spreads and bias in October and February and lower in March and July is evident in both proxy year selections and the Monte-Carlo method. This underscores the role of localization when making model-observation comparisons and suggests that the CMIP models exhibit regional differences in their ice formation processes, which even out on an Arctic-wide scale. Understanding these differences would help improve the representation of sea ice in GCMs in general.

The regional differences between models and observations may arise due to a variety of factors: *Firstly*, the sea ice albedo feedback processes can be a major influence on seasonal sea ice retreat. (Kashiwase et al., 2017; Thackeray and Hall, 2019). *Secondly*, the enhanced heat loss from seawater during the melting season can accelerate the sea ice growth rate later in the season (Bitz and Roe, 2004; Hezel et al., 2012). *Thirdly*, the complexity of ice-ocean feedback processes related to salinity and the sea-surface temperatures can complicate the SIT responses to warming climate (Zhang et al., 2018; Goosse and Zunz, 2014). *Lastly,* temperature and salinity biases due to the excessively deep and thick Atlantic Water layer (Khosravi et al., 2022), along with biases in regional atmospheric temperatures, sea-ice convergence and regional surface wind inconsistencies in CMIP6 models (Crawford et al., 2023), may account for biases in SIT simulations. Moreover, unresolved processes in snow cover may also impact the representation of SIT. For example, the selected CMIP6 models use a uniform snow distribution over their thickness categories. Yet studies have shown that snow is not uniformly distributed over the various ice thickness categories but should be varying with the SIT category (Sturm et. al. 2002, Liston 2004, Castro-Morales et al. 2013). In the models, an unrealistic uniformly thick snow over all categories could lead to overly insulated thin ice layers, explaining some of the underestimated ice growth seen in Fig.8. Overall, the surplus snow in the model simulation might contribute to reduced SIT growth during late winter–early spring months, particularly evident in OpenIFS/FESOM2 when compared to the observations (Fig.7).

Increasing model resolution and properly choosing sea ice model physics would have potential to improve sea ice simulations. A quantitative analysis to distinguish sea ice's thermodynamic and dynamic processes might help improve models and also our understanding of the future Arctic climate and sea ice projections. Future studies will address this.

6. Conclusions

While GCMs are not designed to replicate observations, their ability to reproduce the current polar climate can nevertheless give certain confidence in the projection of the future evolution of sea ice cover (Notz 2015). Yet, evaluating the skill of GCMs with short-term observational campaigns is challenging. This study proposes two proxy year-based approaches to perform meaningful model-observation comparisons for two key parameters of the Arctic system: the sea-ice and snow thicknesses. With this new evaluation methodology, we demonstrate our efforts to address challenges that are typically encountered when comparing GCM outputs to *in-situ* observations: (i) the difference in spatial coverage of the model values in comparison to the observations, (ii)

https://doi.org/10.5194/egusphere-2024-2214
Preprint. Discussion started: 4 September 2024

the fact that the observations are drifting with the sea ice during the year, and (iii) the models' inability to simulate specific observed years.

Firstly, to address the difference in the spatial disparity between the model values and observations, we considered an extensive set of MOSAIC observations deployed within a 40 km radius, comparable to the scale of a GCM grid. *Secondly*, following previous studies employing operational or nudged model data (e.g. Athanase et al. 2019; Pithan et al. 2023), we collocated the CMIP6 model data with observations from each month or day to address the spatial displacement of the observations. *Finally*, we addressed the CMIP6 models' inability to simulate specific years by proposing for the first time "proxy years" of the observed conditions for meaningful model-observation comparisons based on two broad criteria: one based on the AO index, and other on SIA.

Comparing the two proxy-year selection criteria we find that the SIA-based method yields SIT annual cycles closest to the observations. Annual cycles generated using this criterion exhibited relatively lower biases and narrower inter-model spreads when compared to AO-selected proxy years. Further comparing the two proxy-year methods with nudged simulations highlights whether the latter have skills in capturing the anomalous atmospheric flow and its influence on the sea ice and snow along the MOSAIC drift track. We demonstrate that: (a) the proxy year methods effectively capture the anomalous conditions and realizations of natural variability, and (b) the atmospheric conditions are not the primary contributors to the model biases. Finally, a *validation* experiment was executed to rigorously evaluate the reliability of our proxy year selection criteria which reaffirmed that SIA-based proxy year selections were statistically significant. We emphasize that on monthly timescales, our SIA-based criterion performs equally well as nudged simulations in terms of annual maximum and variations. Our evaluation reveals that neither the selection method nor the nudged simulations could accurately replicate the snow thickness annual cycle observed in-situ during MOSAIC, suggesting unresolved processes in nudged and CMIP6 simulations.

In summary, the CMIP6 models faced challenges in accurately simulating sea-ice and snow thickness in the Arctic due to the complexity of the underlying processes. Nevertheless, our two-novel proxy-year selection methods showed modest enhancements in aligning with observed annual cycles, with the SIA-based criterion yielding the best results. Our results highlight that regardless of the specific (free-running or nudged) model configurations, and of conditions within individual proxy years, the general statements about biases in SIT and snow thickness remain consistent. These biases most likely originate from an overly uniform winter snow accumulation and a too rapid snow and sea ice melt. Exploring modeled processes which shape the sea-ice-snow thickness patterns in depth, in particular the mechanisms suggested hereinabove, might offer insights into such accumulation and melting biases. Moreover, extending the

https://doi.org/10.5194/egusphere-2024-2214
Preprint. Discussion started: 4 September 2024

evaluation of model simulations to other datasets, such as observations from Operation IceBridge (Kurtz and Harbeck, 2015) and ICESat-2 (Kacimi and Kwok, 2022), would help test our findings in other atmospheric and sea-ice conditions.

Our study introduces a novel proxy-year selection method for model-observation comparisons, highlighting model biases in simulating Arctic sea ice and reflecting upon their underlying processes. This initial step is crucial to evaluate the performance of CMIP6 models and to identify areas for further improvement. Our results demonstrate that meaningful model evaluation of free-running simulations can be carried out using *in-situ* datasets with important temporal and spatial constraints, even under strongly anomalous observed conditions. Better representation of processes driving the SIT and snow thickness – such as snowfall, snow thinning and redistribution mechanisms, or albedo – will be instrumental in the next generation of GCMs.

https://doi.org/10.5194/egusphere-2024-2214
Preprint. Discussion started: 4 September 2024

Data Availability Statement

The observed Sea-ice Area dataset used in the study is Ocean and Sea-Ice Satellite Application Facility (OSI-SAF) in the European Organisation for the Exploitation of Meteorological Satellites (EUMETSAT) which is available at https://osisaf-hl.met.no/archive/osisaf/sea-ice-index/v2p2/: nh, last accessed: 14.10.2022. All the CMIP6 model datasets are available at ESGF website: https://esgf-node.llnl.gov/search/cmip6/ (Table 1). The observed AO Index has been obtained from NOAA's Climate Prediction Center which can be accessed at https://www.cpc.ncep.noaa.gov/products/precip/CWlink/daily_ao_index/ao.shtml, last accessed 12.07.2023. Data from ECHAM/FESOM and OpenIFS/FESOM2 nudged simulations are available online (https://zenodo.org/records/10133887).

Author contributions

Conceptualized the study: TS, IS and ST
Carried out the analysis and prepared the original draft: All authors.
Provided ideas in an enriching exchange: TS, IS, MA
Contributed to the data curation: IS, MA, ST
Carried out and analyzed the nudged simulations: MA and ASB
Reviewed and contributed to the final draft: All authors.

Acknowledgements

This work was developed as a part of the *"Arctic Processes in CMIP6 Bootcamp"* in October 2022 at Søminestationen, Denmark. We would like to acknowledge the Danish Meteorological Institute, NORP and Clivar/Clic for organizing it. We would also like to extend our acknowledgement to Tina Odaka for managing and making us equipped with Pangeo EOSC Infrastructure (EGI-ACE).

Funding information:

Imke Sievers was funded by the Danish State through the National Center for Climate Research (NCKF). Antonio Sanchez-Benitez was supported by funding from the Helmholtz Research Field Earth & Environment for the Innovation Pool Project SCENIC. This work used resources of the Deutsches Klimarechenzentrum (DKRZ) granted by its Scientific Steering Committee (WLA) under project ID ba1264.

Competing Interests

The authors declare that they have no conflict of interest.

https://doi.org/10.5194/egusphere-2024-2214
Preprint. Discussion started: 4 September 2024

References:

Alfred-Wegener-Institut Helmholtz-Zentrum für Polar- und Meeresforschung: Polar Research and Supply Vessel POLARSTERN Operated by the Alfred-Wegener-Institute, Journal of large-scale research facilities, 3, A119, https://doi.org/10.17815/jlsrf-3-1631, 2017.

Athanase, M., Sennéchael, N., Garric, G., Koenig, Z., Boles, E., & Provost, C.: New hydrographic measurements of the upper Arctic western Eurasian Basin in 2017 reveal fresher mixed layer and shallower warm layer than 2005–2012 climatology. Journal of Geophysical Research: Oceans, 124(2), 1091-1114, 2019.

Bentsen, Mats; Oliviè, Dirk Jan Leo; Seland, Øyvind; Toniazzo, Thomas; Gjermundsen, Ada; Graff, Lise Seland; Debernard, Jens Boldingh; Gupta, Alok Kumar; He, Yanchun; Kirkevåg, Alf; Schwinger, Jörg; Tjiputra, Jerry; Aas, Kjetil Schanke; Bethke, Ingo; Fan, Yuanchao; Griesfeller, Jan; Grini, Alf; Guo, Chuncheng; Ilicak, Mehmet; Karset, Inger Helene Hafsahl; Landgren, Oskar Andreas; Liakka, Johan; Moseid, Kine Onsum; Nummelin, Aleksi; Spensberger, Clemens; Tang, Hui; Zhang, Zhongshi; Heinze, Christoph; Iversen, Trond; Schulz, Michael : NCC NorESM2-MM model output prepared for CMIP6 CMIP historical. Version YYYYMMDD[1].Earth System Grid Federation. https://doi.org/10.22033/ESGF/CMIP6.8040, 2019

Bitz, C.M. and Roe, G.H.: A mechanism for the high rate of sea ice thinning in the Arctic Ocean. Journal of Climate, 17(18), pp.3623-3632, 2004.

Blanchard-Wrigglesworth, E., Farrell, S.L., Newman, T. and Bitz, C.M.: Snow cover on Arctic sea ice in observations and an Earth System Model. Geophysical Research Letters, 42(23), pp.10-342, 2015.

Blanchard-Wrigglesworth, E., Webster, M.A., Farrell, S.L. and Bitz, C.M.: Reconstruction of snow on Arctic sea ice. Journal of Geophysical Research: Oceans, 123(5), pp.3588-3602, 2018.

Bushuk, M., Msadek, R., Winton, M., Vecchi, G.A., Gudgel, R., Rosati, A. and Yang, X.: Skillful regional prediction of Arctic sea ice on seasonal timescales. Geophysical Research Letters, 44(10), pp.4953-4964, 2017.

Castro-Morales, K., Kauker, F., Losch, M., Hendricks, S., Riemann-Campe, K. and Gerdes, R.: Sensitivity of simulated Arctic sea ice to realistic ice thickness distributions and snow parameterizations. Journal of Geophysical Research: Oceans, 119(1), pp.559-571, 2014.

Castro-Morales, K., Ricker, R. and Gerdes, R.: Regional distribution and variability of model-simulated Arctic snow on sea ice. Polar Science, 13, pp.33-49, 2017.

Chen, S., Liu, J., Ding, Y., Zhang, Y., Cheng, X. and Hu, Y.: Assessment of snow depth over Arctic sea ice in CMIP6 models using satellite data. Advances in Atmospheric Sciences, 38, pp.168-186, 2021.

Chen, L., Wu, R., Shu, Q., Min, C., Yang, Q. and Han, B.: The Arctic Sea Ice Thickness Change in CMIP6's Historical Simulations. Advances in Atmospheric Sciences, pp.1-13, 2023.

Clemens-Sewall, D., Polashenski, C., Frey, M.M., Cox, C.J., Granskog, M.A., Macfarlane, A.R., Fons, S.W., Schmale, J., Hutchings, J.K., von Albedyll, L. and Arndt, S.: Snow loss into leads in Arctic sea ice: Minimal in typical wintertime conditions, but high during a warm and windy snowfall event. Geophysical Research Letters, 50(12), p.e2023GL102816, 2023.

https://doi.org/10.5194/egusphere-2024-2214
Preprint. Discussion started: 4 September 2024

Crawford, A.D., Rosenblum, E., Lukovich, J.V. and Stroeve, J.C.: Sources of seasonal sea-ice bias for CMIP6 models in the Hudson Bay Complex. Annals of Glaciology, pp.1-18, 2023.

Danabasoglu, Gokhan: NCAR CESM2 model output prepared for CMIP6 CMIP historical. Version YYYYMMDD[1].Earth System Grid Federation. https://doi.org/10.22033/ESGF/CMIP6.7627, 2019

Danilov, S., Wang, Q., Timmermann, R., Iakovlev, N., Sidorenko, D., Kimmritz, M., Jung, T. and Schröter, J.: Finite-element sea ice model (FESIM), version 2. Geoscientific Model Development, 8(6), pp.1747-1761, 2015.

Danilov, S., Sidorenko, D., Wang, Q. and Jung, T.: The finite-volume sea ice–ocean model (fesom2). Geoscientific Model Development, 10(2), pp.765-789 , 2017.

Day, J.J., Hargreaves, J.C., Annan, J.D. and Abe-Ouchi, A.: Sources of multi-decadal variability in Arctic sea ice extent. Environmental Research Letters, 7(3), p.034011, 2012.

ECMWF: IFS Documentation CY43R3 – Part III: Dynamics and numerical procedures, no. 3 in IFS Documentation, ECMWF, https://doi.org/10.21957/8l7miod5m, 2017.

Eyring, V., Bony, S., Meehl, G.A., Senior, C.A., Stevens, B., Stouffer, R.J. and Taylor, K.E.: Overview of the Coupled Model Intercomparison Project Phase 6 (CMIP6) experimental design and organization. Geoscientific Model Development, 9(5), pp.1937-1958, 2016.

Goosse, H. and Zunz, V.: Decadal trends in the Antarctic sea ice extent ultimately controlled by ice–ocean feedback. The Cryosphere, 8(2), pp.453-470, 2014.

Graham, R.M., Itkin, P., Meyer, A., Sundfjord, A., Spreen, G., Smedsrud, L.H., Liston, G.E., Cheng, B., Cohen, L., Divine, D. and Fer, I.: Winter storms accelerate the demise of sea ice in the Atlantic sector of the Arctic Ocean. Scientific Reports, 9(1), p.9222, 2019.

Gupta, M., Marshall, J., Song, H., Campin, J.M. and Meneghello, G.: Sea-ice melt driven by ice-ocean stresses on the mesoscale. Journal of Geophysical Research: Oceans, 125(11), p.e2020JC016404, 2020.

He, L., Xue, B., Hui, F. and Cheng, X.: Triple Collocation-Based Merging of Winter Snow Depth Retrievals on Arctic Sea Ice Derived From Three Different Algorithms Using AMSR2. IEEE Transactions on Geoscience and Remote Sensing, 2023.

Hezel, P.J., Zhang, X., Bitz, C.M., Kelly, B.P. and Massonnet, F.: Projected decline in spring snow depth on Arctic sea ice caused by progressively later autumn open ocean freeze-up this century. Geophysical Research Letters, 39(17), 2012.

Hu, C., Yang, S., Wu, Q., Li, Z., Chen, J., Deng, K., Zhang, T. and Zhang, C.: Shifting El Niño inhibits summer Arctic warming and Arctic sea-ice melting over the Canada Basin. Nature Communications, 7(1), p.11721, 2016

Hunke, E.C., Lipscomb, W.H. and Turner, A.K.: Sea-ice models for climate study: retrospective and new directions. Journal of Glaciology, 56(200), pp.1162-1172, 2010.

Jackson, K., J. Wilkinson, T. Maksym, D. Meldrum, J. Beckers, C. Haas, and D. Mackenzie: A Novel and Low-Cost Sea Ice Mass Balance Buoy. J. Atmos. Oceanic Technol., **30**, 2676–2688, https://doi.org/10.1175/JTECH-D-13-00058.1, 2013.

https://doi.org/10.5194/egusphere-2024-2214
Preprint. Discussion started: 4 September 2024

Kacimi, S. and Kwok, R.: Arctic Snow Depth, Ice Thickness, and Volume From ICESat-2 and CryoSat-2: 2018–2021. Geophysical Research Letters, 49(5), p.e2021GL097448, 2022.

Kashiwase, H., Ohshima, K.I., Nihashi, S. and Eicken, H.: Evidence for ice-ocean albedo feedback in the Arctic Ocean shifting to a seasonal ice zone. Scientific Reports, 7(1), p.8170, 2017.

Khosravi, N., Wang, Q., Koldunov, N., Hinrichs, C., Semmler, T., Danilov, S. and Jung, T.: The Arctic Ocean in CMIP6 models: Biases and projected changes in temperature and salinity. Earth's Future, 10(2), p.e2021EF002282, 2022.

Koenig, Z., Provost, C., Villacieros-Robineau, N., Sennéchael, N., Meyer, A., Lellouche, J. M., & Garric, G.: Atlantic waters inflow north of Svalbard: Insights from IAOOS observations and Mercator Ocean global operational system during N-ICE 2015. Journal of Geophysical Research: Oceans, 122(2), 1254-1273, 2017.

Kouki, K., Räisänen, P., Luojus, K., Luomaranta, A. and Riihelä, A.: Evaluation of Northern Hemisphere snow water equivalent in CMIP6 models during 1982–2014. The Cryosphere, 16(3), pp.1007-1030.Kurtz, N., & Harbeck, J., 2015. Operation IceBridge sea ice freeboard, snow depth, and thickness data products manual, version 2 processing. NSIDC, Boulder, CO, USA, Tech. Rep, 2022.

Lavergne, T., Sørensen, A.M., Kern, S., Tonboe, R., Notz, D., Aaboe, S., Bell, L., Dybkjær, G., Eastwood, S., Gabarro, C. and Heygster, G.: Version 2 of the EUMETSAT OSI SAF and ESA CCI sea-ice concentration climate data records. The Cryosphere, 13(1), pp.49-78, 2019.

Lei, R., Cheng, B., Hoppmann, M. and Zuo, G.: Snow depth and sea ice thickness derived from the measurements of SIMBA buoys deployed in the Arctic Ocean during the Legs 1a, 1, and 3 of the MOSAiC campaign in 2019-2020. PANGAEA. DOI: http://dx. doi. org/10.1594/PANGAEA, 938244, 2021.

Liston, G. E.: Representing Subgrid Snow Cover Heterogeneities in Regional and Global Models. J. Climate, 17, 1381–1397, https://doi.org/10.1175/1520-0442(2004)017<1381:RSSCHI>2.0.CO;2, 2004.

Losch, M., Menemenlis, D., Campin, J.M., Heimbach, P. and Hill, C.: On the formulation of sea-ice models. Part 1: Effects of different solver implementations and parameterizations. Ocean Modelling, 33(1-2), pp.129-144, 2010.

Macfarlane, A.R., Schneebeli, M., Dadic, R., Tavri, A., Immerz, A., Polashenski, C., Krampe, D., Clemens-Sewall, D., Wagner, D.N., Perovich, D.K. and Henna-Reetta, H.: a Database of Snow on Sea Ice in the Central arctic Collected during the MOSAiC expedition. Scientific Data, 10(1), p.398, 2023.

MacGregor, J.A., Boisvert, L.N., Medley, B., Petty, A.A., Harbeck, J.P., Bell, R.E., Blair, J.B., Blanchard-Wrigglesworth, E., Buckley, E.M., Christoffersen, M.S. and Cochran, J.R.: The scientific legacy of NASA's Operation IceBridge, 2021.

Manucharyan, G.E. and Thompson, A.F.: Submesoscale sea ice-ocean interactions in marginal ice zones. Journal of Geophysical Research: Oceans, 122(12), pp.9455-9475, 2017.

Neubauer, David; Ferrachat, Sylvaine; Siegenthaler-Le Drian, Colombe; Stoll, Jens; Folini, Doris Sylvia; Tegen, Ina; Wieners, Karl-Hermann; Mauritsen, Thorsten; Stemmler, Irene; Barthel, Stefan; Bey, Isabelle; Daskalakis, Nikos; Heinold, Bernd; Kokkola, Harri; Partridge, Daniel; Rast, Sebastian; Schmidt, Hauke; Schutgens, Nick; Stanelle, Tanja; Stier, Philip; Watson-Parris, Duncan; Lohmann, Ulrike.: HAMMOZ-

https://doi.org/10.5194/egusphere-2024-2214
Preprint. Discussion started: 4 September 2024

Consortium MPI-ESM1.2-HAM model output prepared for CMIP6 CMIP historical. Version YYYYMMDD[1].Earth System Grid Federation. https://doi.org/10.22033/ESGF/CMIP6.5016, 2019.

Nicolaus, M et al.: Snow height on sea ice, meteorological conditions and drift of sea ice from autonomous Snow Buoys during MOSAiC 2019/20. PANGAEA, https://doi.pangaea.de/10.1594/PANGAEA.933742, 2021 [dataset in review]

Nicolaus, M., Hoppmann, M., Arndt, S., Hendricks, S., Katlein, C., Nicolaus, A., Rossmann, L., Schiller, M. and Schwegmann, S.: Snow depth and air temperature seasonality on sea ice derived from snow buoy measurements. Frontiers in Marine Science, 8, p.655446, 2021.

Nicolaus, M., Perovich, D.K., Spreen, G., Granskog, M.A., von Albedyll, L., Angelopoulos, M., Anhaus, P., Arndt, S., Belter, H.J., Bessonov, V. and Birnbaum, G.: Overview of the MOSAiC expedition: Snow and sea ice. Elem Sci Anth, 10(1), p.000046, 2022.

Notz, D.: How well must climate models agree with observations?. Philosophical Transactions of the Royal Society A: Mathematical, Physical and Engineering Sciences, 373(2052), p.20140164, 2015.

Notz, D., Jahn, A., Holland, M., Hunke, E., Massonnet, F., Stroeve, J., Tremblay, B. and Vancoppenolle, M.: The CMIP6 Sea-Ice Model Intercomparison Project (SIMIP): understanding sea ice through climate-model simulations. Geoscientific Model Development, 9(9), pp.3427-3446, 2016.

Notz, D., & Community, S. I. M. I. P.: Arctic sea ice in CMIP6. Geophysical Research Letters, 47(10), e2019GL086749, 2020.

Ogi, M., Yamazaki, K. and Wallace, J.M.: Influence of winter and summer surface wind anomalies on summer Arctic sea ice extent. Geophysical Research Letters, 37(7) , 2010..

Perovich, D.K., Grenfell, T.C., Light, B. and Hobbs, P.V.:Seasonal evolution of the albedo of multiyear Arctic sea ice. Journal of Geophysical Research: Oceans, 107(C10), pp.SHE-20, 2002.

Pithan, F., Athanase, M., Dahlke, S., Sánchez-Benítez, A., Shupe, M.D., Sledd, A., Streffing, J., Svensson, G. and Jung, T.: Nudging allows direct evaluation of coupled climate models with in-situ observations: A case study from the MOSAiC expedition. EGUsphere, pp.1-23, 2022.

Rabe, B., Cox, C. J., Fang, Y. C., Goessling, H., Granskog, M. A., Hoppmann, M., ... & Zuo, G.: The MOSAiC Distributed Network: Observing the coupled Arctic system with multidisciplinary, coordinated platforms. Elementa: Science of the Anthropocene, 12(1) , 2024.

Rabe, B., Heuzé, C., Regnery, J., Aksenov, Y., Allerholt, J., Athanase, M., Bai, Y., Basque, C., Bauch, D., Baumann, T.M. and Chen, D.: Overview of the MOSAiC expedition: Physical oceanography. Elem Sci Anth, 10(1), p.00062, 2022.

Rackow, T., Goessling, H.F., Jung, T., Sidorenko, D., Semmler, T., Barbi, D. and Handorf, D.: Towards multi-resolution global climate modeling with ECHAM6-FESOM. Part II: climate variability. Climate dynamics, 50, pp.2369-2394, 2018.

Rigor, I.G., Wallace, J.M. and Colony, R.L.: Response of sea ice to the Arctic Oscillation. Journal of Climate, 15(18), pp.2648-2663, 2002.

Roach, L.A., Dörr, J., Holmes, C.R., Massonnet, F., Blockley, E.W., Notz, D., Rackow, T., Raphael, M.N., O'Farrell, S.P., Bailey, D.A. and Bitz, C.M.: Antarctic sea ice area in CMIP6. Geophysical Research Letters, 47(9), p.e2019GL086729, 2020.

https://doi.org/10.5194/egusphere-2024-2214
Preprint. Discussion started: 4 September 2024

Sánchez-Benítez, A., Goessling, H., Pithan, F., Semmler, T. and Jung, T.: The July 2019 European heat wave in a warmer climate: storyline scenarios with a coupled model using spectral nudging. Journal of Climate, 35(8), pp.2373-2390, 2022.

Seland, Øyvind; Bentsen, Mats; Oliviè, Dirk Jan Leo; Toniazzo, Thomas; Gjermundsen, Ada; Graff, Lise Seland; Debernard, Jens Boldingh; Gupta, Alok Kumar; He, Yanchun; Kirkevåg, Alf; Schwinger, Jörg; Tjiputra, Jerry; Aas, Kjetil Schanke; Bethke, Ingo; Fan, Yuanchao; Griesfeller, Jan; Grini, Alf; Guo, Chuncheng; Ilicak, Mehmet; Karset, Inger Helene Hafsahl; Landgren, Oskar Andreas; Liakka, Johan; Moseid, Kine Onsum; Nummelin, Aleksi; Spensberger, Clemens; Tang, Hui; Zhang, Zhongshi; Heinze, Christoph; Iversen, Trond; Schulz, Michael.: NCC NorESM2-LM model output prepared for CMIP6 CMIP historical. Version YYYYMMDD[1].Earth System Grid Federation. https://doi.org/10.22033/ESGF/CMIP6.8036, 2019.

Seland, Ø., Bentsen, M., Olivié, D., Toniazzo, T., Gjermundsen, A., Graff, L.S., Debernard, J.B., Gupta, A.K., He, Y.C., Kirkevåg, A. and Schwinger, J.: Overview of the Norwegian Earth System Model (NorESM2) and key climate response of CMIP6 DECK, historical, and scenario simulations. Geoscientific Model Development, 13(12), pp.6165-6200, 2020.

Semmler, Tido; Danilov, Sergey; Rackow, Thomas; Sidorenko, Dmitry; Barbi, Dirk; Hegewald, Jan; Sein, Dmitri; Wang, Qiang; Jung, Thomas.: AWI AWI-CM1.1MR model output prepared for CMIP6 CMIP. Version YYYYMMDD[1].Earth System Grid Federation. https://doi.org/10.22033/ESGF/CMIP6.359, 2018.

Semmler, T., Danilov, S., Gierz, P., Goessling, H.F., Hegewald, J., Hinrichs, C., Koldunov, N., Khosravi, N., Mu, L., Rackow, T. and Sein, D.V.: Simulations for CMIP6 with the AWI climate model AWI-CM-1-1. Journal of Advances in Modeling Earth Systems, 12(9), p.e2019MS002009, 2020.

Shen, Z., Duan, A., Li, D. and Li, J.: Assessment and ranking of climate models in Arctic Sea ice cover simulation: From CMIP5 to CMIP6. Journal of Climate, 34(9), pp.3609-3627, 2021.

Shu, Q., Wang, Q., Song, Z., Qiao, F., Zhao, J., Chu, M. and Li, X.: Assessment of sea ice extent in CMIP6 with comparison to observations and CMIP5. Geophysical Research Letters, 47(9), p.e2020GL087965, 2020.

Shupe, M.D., Rex, M., Blomquist, B., Persson, P.O.G., Schmale, J., Uttal, T., Althausen, D., Angot, H., Archer, S., Bariteau, L. and Beck, I.: Overview of the MOSAiC expedition: Atmosphere. Elem Sci Anth, 10(1), p.00060, 2022.

Sidorenko, D., Rackow, T., Jung, T., Semmler, T., Barbi, D., Danilov, S., Dethloff, K., Dorn, W., Fieg, K., Gößling, H.F. and Handorf, D.: Towards multi-resolution global climate modeling with ECHAM6–FESOM. Part I: model formulation and mean climate. Climate Dynamics, 44, pp.757-780, 2015.

Stevens, B., and Coauthors: Atmospheric component of the MPI-M Earth system model: ECHAM6. Journal of Advances in Modeling Earth Systems, 5, 146–172, https://doi.org/10.1002/jame.20015, 2013.

Streffing, J., Sidorenko, D., Semmler, T., Zampieri, L., Scholz, P., Andrés-Martínez, M., Koldunov, N., Rackow, T., Kjellsson, J., Goessling, H. and Athanase, M.: AWI-CM3 coupled climate model: description and evaluation experiments for a prototype post-CMIP6 model. Geoscientific Model Development, 15(16), pp.6399-6427, 2022.

https://doi.org/10.5194/egusphere-2024-2214
Preprint. Discussion started: 4 September 2024

Sturm, M., Holmgren, J. and Perovich, D.K.: Winter snow cover on the sea ice of the Arctic Ocean at the Surface Heat Budget of the Arctic Ocean (SHEBA): Temporal evolution and spatial variability. Journal of Geophysical Research: Oceans, 107(C10), pp.SHE-23, 2002.

Svensson, G., Murto, S., Shupe, M. D., Pithan, F., Magnusson, L., Day, J. J., ... & Vihma, T.: Warm air intrusions reaching the MOSAiC expedition in April 2020—The YOPP targeted observing period (TOP). Elementa: Science of the Anthropocene, 11(1), 2022.

Thackeray, C.W. and Hall, A.: An emergent constraint on future Arctic sea-ice albedo feedback. Nature Climate Change, 9(12), pp.972-978, 2019.

von Storch, Jin-Song; Putrasahan, Dian; Lohmann, Katja; Gutjahr, Oliver; Jungclaus, Johann; Bittner, Matthias; Haak, Helmuth; Wieners, Karl-Hermann; Giorgetta, Marco; Reick, Christian; Esch, Monika; Gayler, Veronika; de Vrese, Philipp; Raddatz, Thomas; Mauritsen, Thorsten; Behrens, Jörg; Brovkin, Victor; Claussen, Martin; Crueger, Traute; Fast, Irina; Fiedler, Stephanie; Hagemann, Stefan; Hohenegger, Cathy; Jahns, Thomas; Kloster, Silvia; Kinne, Stefan; Lasslop, Gitta; Kornblueh, Luis; Marotzke, Jochem; Matei, Daniela; Meraner, Katharina; Mikolajewicz, Uwe; Modali, Kameswarrao; Müller, Wolfgang; Nabel, Julia; Notz, Dirk; Peters-von Gehlen, Karsten; Pincus, Robert; Pohlmann, Holger; Pongratz, Julia; Rast, Sebastian; Schmidt, Hauke; Schnur, Reiner; Schulzweida, Uwe; Six, Katharina; Stevens, Bjorn; Voigt, Aiko; Roeckner, Erich.: MPI-M MPIESM1.2-HR model output prepared for CMIP6 HighResMIP. Version YYYYMMDD[1].Earth System Grid Federation. https://doi.org/10.22033/ESGF/CMIP6.762, 2017.

Wagner, D.N., Shupe, M.D., Cox, C., Persson, O.G., Uttal, T., Frey, M.M., Kirchgaessner, A., Schneebeli, M., Jaggi, M., Macfarlane, A.R. and Itkin, P.: Snowfall and snow accumulation during the MOSAiC winter and spring seasons. The Cryosphere, 16(6), pp.2373-2402, 2022.

Wang, Q., Danilov, S., Sidorenko, D., Timmermann, R., Wekerle, C., Wang, X., Jung, T. and Schröter, J.: The Finite Element Sea Ice-Ocean Model (FESOM) v. 1.4: formulation of an ocean general circulation model. Geoscientific Model Development, 7(2), pp.663-693, 2014.

Warren, S. G., I. G. Rigor, N. Untersteiner, V. F. Radionov, N. N. Bryazgin, Y. I. Aleksandrov, and R. Colony: Snow Depth on Arctic Sea Ice. J. Climate, **12**, 1814–1829, https://doi.org/10.1175/1520-0442(1999)012<1814:SDOASI>2.0.CO;2, 1999.

Watts, M., Maslowski, W., Lee, Y. J., Kinney, J. C., & Osinski, R.: A spatial evaluation of Arctic sea ice and regional limitations in CMIP6 historical simulations. Journal of Climate, 34(15), 6399-6420, 2021.

Webster, M., Gerland, S., Holland, M., Hunke, E., Kwok, R., Lecomte, O., Massom, R., Perovich, D. and Sturm, M.: Snow in the changing sea-ice systems. Nature Climate Change, 8(11), pp.946-953, 2018.

Webster, M.A., DuVivier, A.K., Holland, M.M. and Bailey, D.A.: Snow on Arctic sea ice in a warming climate as simulated in CESM. Journal of Geophysical Research: Oceans, 126(1), p.e2020JC016308, 2021.

Wei, J., Zhang, X. and Wang, Z.: Reexamination of Fram Strait sea ice export and its role in recently accelerated Arctic sea ice retreat. Climate Dynamics, 53(3-4), pp.1823-1841, 2019.

West, A., Blockley, E. and Collins, M.: Understanding model spread in sea ice volume by attribution of model differences in seasonal ice growth and melt. The Cryosphere, 16(10), pp.4013-4032, 2022.

https://doi.org/10.5194/egusphere-2024-2214
Preprint. Discussion started: 4 September 2024

Wieners, Karl-Hermann; Giorgetta, Marco; Jungclaus, Johann; Reick, Christian; Esch, Monika; Bittner, Matthias; Legutke, Stephanie; Schupfner, Martin; Wachsmann, Fabian; Gayler, Veronika; Haak, Helmuth; de Vrese, Philipp; Raddatz, Thomas; Mauritsen, Thorsten; von Storch, Jin-Song; Behrens, Jörg; Brovkin, Victor; Claussen, Martin; Crueger, Traute; Fast, Irina; Fiedler, Stephanie; Hagemann, Stefan; Hohenegger, Cathy; Jahns, Thomas; Kloster, Silvia; Kinne, Stefan; Lasslop, Gitta; Kornblueh, Luis; Marotzke, Jochem; Matei, Daniela; Meraner, Katharina; Mikolajewicz, Uwe; Modali, Kameswarrao; Müller, Wolfgang; Nabel, Julia; Notz, Dirk; Peters-von Gehlen, Karsten; Pincus, Robert; Pohlmann, Holger; Pongratz, Julia; Rast, Sebastian; Schmidt, Hauke; Schnur, Reiner; Schulzweida, Uwe; Six, Katharina; Stevens, Bjorn; Voigt, Aiko; Roeckner, Erich: MPI-M MPI-ESM1.2-LR model output prepared for CMIP6 CMIP historical. Version YYYYMMDD[1].Earth System Grid Federation. https://doi.org/10.22033/ESGF/CMIP6.6595, 2019.

Willatt, R. C., Giles, K. A., Laxon, S. W., Stone-Drake, L., & Worby, A. P.: Field Investigations of Ku-Band Radar Penetration Into Snow Cover on Antarctic Sea Ice. IEEE Transactions on Geoscience and Remote Sensing, 48(1), 365–372. https://doi.org/10.1109/TGRS.2009.2028237, 2010.

Winkelbauer, S., Mayer, M. & Haimberger, L.: Validation of key Arctic energy and water budget components in CMIP6. Clim Dyn **62**, 3891–3926. https://doi.org/10.1007/s00382-024-07105-5, 2024.

Xu, M., & Li, J.: Assessment of sea ice thickness simulations in the CMIP6 models with CICE components. Frontiers in Marine Science, 10, 1223772, 2023.

Zhang, J., Stegall, S.T. and Zhang, X.: Wind–sea surface temperature–sea ice relationship in the Chukchi–Beaufort Seas during autumn. Environmental Research Letters, 13(3), p.034008, 2018.

Zhou, Lu; Stroeve, Julienne; Xu, Shiming; Petty, Alek; Tilling, Rachel; Winstrup, Mai; Rostosky, Philip; Lawrence, Isobel R.; Liston, Glen E.; Ridout, Andy: Inter-comparison of snow depth over Arctic sea ice from reanalysis reconstructions and satellite retrieval. The Cryosphere, 15(1), 345-367, 2021.